The Brenda Field Development: a Multi-Disciplinary Approach

By

Ian F. Jones[1]
Rod Christensen[2]
Jamie Haynes[3]
John Faragher[1]
Ika Novianti[1]
Henry Morris[3]
Giles Pickering[4]

1: GX Technology, 180 High Street, Egham, Surrey TW20 9DN, UK
2: Oilexco North Sea Ltd., Suite 3200, 715 5th Ave SW, Calgary, AB, T2P 2X6, Canada
3: IKON Science Ltd., 2 Castle Business Village, Station Rd, Hampton, TW12 2BX, UK
4. TROY-IKODA Ltd, The Coach House, 90 Alma Rd, Windsor, SL4 3ET, UK

First Break
v22, No.6, p85-91

Corresponding Author
Ian F. Jones
ijones@gxt.com

The Brenda Field Development, Jones, et al.
First Break, v22, No.6, p85-91

The Brenda Field Development: a Multi-Disciplinary Approach

Ian F. Jones[1], Rod Christensen[2], Jamie Haynes[3], John Faragher[1], Ika Novianti[1],
Henry Morris[3], Giles Pickering[4]

1: GX Technology, 180 High Street, Egham, Surrey TW20 9DN, UK
2: Oilexco North Sea Ltd., Suite 3200, 715 5th Ave SW, Calgary, AB, T2P 2X6, Canada
3: IKON Science Ltd., 2 Castle Business Village, Station Rd, Hampton, TW12 2BX, UK
4. TROY-IKODA Ltd, The Coach House, 90 Alma Rd, Windsor, SL4 3ET, UK

Abstract

Recent initiatives in the North Sea and UKCS such as the introduction of the ‘Fallow Field’ initiative and offering of ‘Promote’ licenses have started to generate activity by attracting new entrants who can provide new capital and new ideas to focus on exploration and appraisal. Fields which had been abandoned, or considered of insufficient commercial interest have been offered a new lease of life by allowing proactive companies to identify and exploit latent commercial prospects by tying in to existing infrastructure.

Here we showcase one such recent discovery, made by Oilexco, where a multi-disciplinary approach was taken to identify potential targets using state-of-the-art pre-processing and high resolution velocity model building and pre-stack imaging, combined with detailed calibrated reservoir attribute analysis based on elastic impedance inversion.

This field could prove to be one of the largest finds in the North Sea in recent years.

Introduction

Oilexco's UK North Sea drilling program on License P1042 (Block 15/25b) in the Outer Moray Firth, targeted oil in the Paleocene Upper Balmoral Sandstone. Initially three wells were proposed:, one on the structure previously drilled by the 15/25b-3 well, one on a structural high with classic four-way closure and one on a channel sand feature, whose prospectivity was indicated by an anomalously low elastic impedance (EI) response on the far-offset stack.

The surface location of the first new well, 15/25b-6 is approximately 150 meters west of Conoco’s 15/25b-3 undeveloped discovery, which tested 2,690 bbl/d of 39 degrees oil from the Upper Balmoral Sandstone from 20 feet of net pay in 1990.

The 15/25b-6 well encountered the "Brenda" oil find announced by Oilexco on January 26 2004. The well intersected a series of oil-bearing Paleocene Upper Balmoral sands, the thickest of which has 26 feet of high quality oil pay. In addition to this sand, several other thin bedded oil bearing sands were also intersected. The entire section was tested and yielded 40 degrees API oil from the Upper Balmoral Sandstone at an average rate of 2,980 bbl/d, over an 18-hour test under stable flowing conditions, from 56 feet of perforations (evaluated with open-hole wire-line logs and formation fluid sampling tools). Associated natural gas flowed at an average rate of 600 Mcf/d throughout the test. No water or sand was produced during the test period.

The surface location of the second well (15/25b-7) is approximately 4 kilometres northwest of 15/25b-6.. The vertical hole encountered ~ 50 feet of good quality Upper Balmoral sand which was logged as water bearing. The side-track (15/25b-7Z) encountered another very porous clean Paleocene Upper Balmoral sand with a thin oil column at the top of the sand and a mud log gas response. The results of the well suggest that the "Sheryl" structure is separate from the "Brenda" oil accumulation which is at a structurally lower position. As a consequence, the well was abandoned

The third well, (15/25b-8) targeted the low EI anomaly. It was located 0.50 kilometres west of the 15/25b-6 well, acting as an appraisal well to the "Brenda" oil accumulation. The well encountered 69ft of high quality oil pay in the Upper Balmoral sand, and also tested 40 degree API oil, but at rates up to 4785 bbl/d.

Geological Setting and Drilling Program

During the Paleocene, the East Shetland and Orkney Platforms were sites of deltaic outbuilding. These platforms were uplifted by significant thermal bulging. The uplifting and over-steepening of the delta and shelf slope systems caused instability and failure resulting in a direct supply of sands and sediments to the basin within density flows. Confined density flows of sand-rich sediment started with erosional scour channels that were not overwhelmed by the volume of sediment supply. These distinct channel fairways mark the sand transport paths. Sands within these meandering channels are characterized as massive sandstones with planar and laminated sandstones and occasional load and dish structures. This type of density flow is common in the later Paleocene (Thanetian) and can generally be recognized by seismic data due to the contrast between the laterally equivalent shales and claystones.

Initially, Oilexco reported that the uppermost Paleocene sand was the Forties Member of the Rogaland Group, however, subsequent biostratigraphic analysis has placed this sand within the Upper Balmoral Member of the Montrose Group.

The depositional profile was demonstrated in a Conoco core display at the 2003 Petroleum Geology Conference, which utilized the 15/12-1 well as illustrative of the shelf. The Balmoral-age sands were deposited in a sand (wave dominated) delta with clean, winnowed sand building up during a highstand. As the delta front was oversteepened, periodic failure occurred which triggered debris flows that traveled up to 25 kilometres. This provided the sand reservoirs at MacCulloch and beyond (figure 1). The cores from the Conoco MacCulloch wells are indicative of sand-rich debris/density flows, similar to the sands Oilexco is seeing within the Upper Balmoral Member in the 15/25b Block. Some of these sand types are described, by Conoco, as upper medium-grained, feldspathic, massive sandstone with very rare faint laminations, oil-saturated, friable to uncemented, very high porosity estimated to 30%, permeability measured from 1 to 2 Darcies.

Oilexco interpreted that the Paleocene Upper Balmoral “density flow” sand was only partially encountered by the Conoco 15/25b-3 well. The channel was nearly 50 feet thick at the nearby Sun Glamis 16/21a-6 well. In the other direction, the 15/24b-6 well in the down-dip portion of the MacCulloch Field contains over 120 feet of the Upper Balmoral Sandstone Member. The 15/25b-3 well encountered only 22 feet of sand. This sand was fine to medium grained, moderately sorted, and friable. The sedimentary structures of this sand were massive with planar laminations and good visible porosity. The entire sand down to the scour was oil stained with uniform yellow fluorescence and fast streaming cut. Core examination of the Conoco 15/25b-3 well allowed Oilexco to question whether or not the oil was trapped structurally or stratigraphically. An oil/water contact was not evident in the Upper Balmoral sand in this core and a possible stratigraphic trapping mechanism was suspected.

The Oilexco 15/25b-6 well location was selected to test the stratigraphic interpretation of the Upper Balmoral sand fairway and was situated about 150 meters from the Conoco 15/25b-3 well. As predicted, the Oilexco 15/26b-6 well encountered a thicker Upper Balmoral sandstone section. A thickness of 60 feet of Upper Balmoral was encountered in the Oilexco well in contrast to the 25 feet of Upper Balmoral section encountered in the Conoco 15/25b-3 well.

Seismic Data Pre-Processing

The main aim of the pre-processing work was to optimally prepare the gathers for imaging, focussing attention through the chalk interval. It was imperative that amplitudes be preserved through the processing sequence, since AVO techniques would be integral in identifying key prospects. Short period water bottom multiples contaminated the data, so great effort was expended in finding the optimum methodology to suppress them. The total re-processed area was some 300 sq.km.

Swell noise contamination and cable noise was found to be a problem on a considerable number of sail-lines throughout the survey; therefore proprietary swell attenuator was tested. The process was found to be extremely effective at minimising swell noise and other anomalous amplitudes while leaving the primary signal untouched.

The presence of steeply dipping noise in shot domain was also noted at this point. The noise had characteristics of “strum”, where a low frequency guided wave is generated along the full length of the cable by the tugging of the paravanes. This is prevalent on the two outer cables. On the basis of the testing results it was decided that the coherent dipping noise would be best handled by application of a dip filter in Tau-P space, and that this would therefore be performed at a later stage of the pre-processing.

Due to the intrinsic limitations of velocities picked prior to migration, it was considered preferable to aim for a pre-migration demultiple method which was non-velocity driven, reducing the risk of attenuation of primary energy to a minimum. A surface related multiple attenuation (SRME) approach was therefore tested. This method is a two step process, the first step being the creation of a multiple estimate of the data, and the second being the matching and subtraction of this from the input data.

Following SRME the data was found to contain a certain amount of residual (interbed) multiple energy which was successfully attenuated by application of deconvolution in Tau-P space. As dip filtering was required in Tau-P space to remove the strum noise, the transform was designed to model only the desired dip ranges.

Velocity Model Building & Pre-Stack Depth Migration

The main focus of the imaging work was to accurately resolve the intricate faulting and small structures around the top chalk marker. Considerable care was taken in determining a detailed velocity model, through gridded tomography techniques, that would honour structural and stratigraphic variations (Jones, 2003). Correct estimation of the overburden and chalk velocities were central to accurate preserved amplitude imaging of the targets.

The initial depth interval velocity was built from the time-RMS stacking velocity and converted to depth interval velocity. The water bottom was picked and gridded, based on an initial migration to create the water layer in the depth interval velocity model.

Following this step, we proceeded to three iterations of gridded tomographic update (Sugrue et al, 2003). Each iteration of our tomographic velocity model update consists of two steps:
1. Dense continuous automatic picking of the migrated seismic gathers to determine the residual moveout correction representative of the velocity perturbation
2. Depth domain tomographic inversion to update the velocity model based on the residual moveout velocity and the local dip-field estimated during the auto-picking.

The autopicker is a proprietary GXT algorithm, based on plane-wave destructors (Claerbout, 1992; Hardy, 2003). A user-defined 3D probe containing trace portions for different CDP's and offsets is moved about the data. At each position, 2 slopes are computed (along the offset and CDP axis) which minimize the amplitude variation in a least square sense. The quality of this estimate is also computed. As a result of this picking, a 3D slope field and residual moveout estimate are determined.

As a by-product of the autopicking, we also obtained a residual move-out (RMO) corrected stack of the image. This is a good indication of whether the autopicker has found the correct residual moveout in preparation for the tomographic update.

Following the autopicking, the tomography takes the RMO and dip field measurements in conjunction with weights based on the ‘quality’ of the autopicks, and generates a tomographic solution to minimize the residual moveout values (make the gathers flat and correctly position the data).

Various QC steps are involved during this iterative process, both for the autopicking and the tomography itself. QC products for velocity updating procedures include displays of image gathers before and after the update, stacks and residual depth error grids. A particularly effective QC in 3D is one whereby the residual depth error is displayed in a 3D volume such that it is transparent when depth error is zero (Hardy, 2003). Figure 2 below shows residual curvature (depth error) for the initial and final model. Figure 3 shows the velocity model superimposed on the seismic, an important check to make sure the velocity updates are geologically plausible.

Following completion of the model building, an amplitude preserving 3D Kirchhoff pre-stack depth migration was performed outputting all gathers on a 25m * 25m grid.

To flatten any residual moveout after the final migration, we also employ the continuous autopicker. For this dataset, the spatially consistent RMO velocity field was output on a 100m x 100m grid.

Following spectral analysis of the stacked data, spectral shaping using a time-variant approach was used to increase the apparent maximum bandwidth of the data considerably, without introducing an unacceptable amount of noise. Figure 4 shows the near and far angle stacks with the spectrum of the target zone, over the MacCulloch filed.

Reservoir Characterisation

On the MacCulloch field, 12 km NW of Brenda, Conoco have noted that the seismic event representing the top of the reservoir is characterized by a “Class III” (weak trough – near offset, strong trough – far offset) AVO anomaly (Scorer, et al, 2003). Scorer claims that this technique has been a good “oil indicator” with an oil/water contact evident. Oil production and hence the substitution of oil for water “hardens” the top reservoir response with time-lapse effects being most marked on the far offset data. They note that structural closure does not explain the trap at the MacCulloch Field, and that the field trapping mechanism is stratigraphic. The evidence of a stratigraphic trap is demonstrated with their AVO impedance maps that illustrate where the “oil effect” terminates. This is the same type of anomaly that Oilexco is following in the “Brenda” area.

Here, the data were split into two partial angle stacks (0-25° and 25-50°) to be analysed separately. The gathers show some systematic variation of amplitude with offset, which is particularly clear with some filtering, and appeared to conform to the expected seismic responses predicted by the well data. Top Balder and Top Chalk horizons were picked. Ideally a pick at the top reservoir would also have been made, however, this was not practical as the modelling and subsequent well ties suggests there may be polarity reversals between near and far offset data depending on both porosity and saturation. Furthermore, the sandstone thickness varies, making it more complicated to pick the top of the event.

Average absolute amplitude maps were made over an interval 50ms to 200ms below the Top Balder (Figure 5). The main channel meandering SE from MacCulloch shows up well on both near and far stack data. On the far stack data parts of the two producing fields (MacCulloch and Blenheim) show up as bright anomalies. Also shown up as bright anomalies are parts of the main channel, in particular the section to the West and South of 15/25b-3. These far stack anomalies are illustrated by the example seismic lines shown in Figures 6 for the MacCulloch Field and figure 7 for the Blenheim field and Brenda discovery.

Wavelet extraction and well ties

Inversion of seismic data is designed to produce an impedance volume from a seismic data set. A well inverted impedance volume should be a good estimate of the rock properties, enabling better prediction characterisation of the reservoir. A standard reflection seismic data set can be modelled as a convolution of the vertical series of rock properties with a seismic wavelet and some level of noise. Inversion requires the extraction of this wavelet, to invert the seismic back to the rock properties. The frequency content of both the near and far angle stacks was analysed and wavelets produced.

The near stack wavelet was then used, along with the logs and check-shot survey, to produce synthetic seismograms at the well locations. The synthetic seismogram shows a good match with the near stack data in both MacCulloch wells. It was noted that the data is not capable of resolving thin sands, but a sand response is indicated for the thicker sand in 15/24b-6. Prediction of the expected response at the far stack was made by using AVO modelling, shown for 15/24b-6 in figure 8.

Seismic inversion of near and far stacks

In addition to the wavelet and the seismic data, the other main input to the inversion process is a background impedance model. This is required to estimate an absolute impedance, as the seismic data contains no low (<5 Hz) frequency information. This model is built by interpolating the appropriate well logs across the area, using the picked horizons, and then smoothing the resulting model so that only those frequencies that do not lie within the seismic data remain. Models were built using the EI15 logs for the near stack inversion and EI38 for the far stack. In addition to the Top Chalk and Top Balder horizons, a Near Oligocene horizon was also picked to provide a better model for the Eocene.

It is worth noting that the underlying assumption is made that the well data adequately represents any variation in the rock properties across the area to be inverted. In this case only three wells were available for use, so the control is limited. There was little evidence of a large systematic variation in the rock properties across the area, however such variations cannot be completely discounted given the small number of wells available.

AVO impedance is an attribute that is designed to optimise the identification of hydrocarbon bearing reservoir by using both near and far impedances together. The underlying principle is to use the two volumes to eliminate the reservoir quality element from the impedance measures, so that the remaining measure is only of the level of hydrocarbon saturation.

Inversion results

As the known hydrocarbon occurrences and other anomalies are most easily seen on the far impedance volume and given the potential problems of the AVO Impedance volume due to inaccuracies in the near stack volume, the interpretation effort focussed on the far impedance. Figures 9a & b show the low EI38 response at the 15/24b-6 well, showing a clear anomaly in the oil bearing zone. Note that the time interval of the seismic has been reduced to the zone around the known reservoirs to assist in the interpretation and visualization.

Figure 10 shows a line through the 15/25a-2 well and figure 11 shows the associated EI results near this well, showing a lower EI zone up-dip from the well, which may indicate that the well penetrated the edge of an accumulation. Figures 12a & b show the EI38 results at the new 15/24b-6 location. It is clear that the old 15/25b-3 well is offset from the main hydrocarbon indicator response. Although the background EI38 appears to increase from 15/24b-6 to 15/25a-2, it could be that the low EI38 values at 15/24b-6, due to the presence of oil, are unduly lowering the background EI38 in the western part of the volume, due to lack of any control points in water saturated sandstone. Potential problems like this illustrate that the inversion process must always be considered when interpreting inversion results.

Analysing the results with a 3D visualization package permits an aerial perspective of those parts of the channel sand system with hydrocarbon potential. “Turning-off” all the voxels with values greater than 525 (g/cc)*(m/s) (figure 13) shows these low EI38 bodies for the area. The major elements are clearly the large series of bodies lying along the channel trend SE of the 15/25a-2 well, and the presence of a body representing the Blenheim field. The presence of the Blenheim body is important, as this constitutes a “blind-test” of the method, as no well data from this field was used in this project. Both the MacCulloch and Blenheim fields show up as having low values of AVO Impedance, demonstrating that this is an indicator of oil-bearing sand. The AVO impedance of the remaining bodies varies from being indicative of oil, to some values that are more indicative of water sands, as anticipated from the relative levels of EI15 and EI38 noted above. However, this could be due to the difficulty in reliably estimating EI15, or a thinning of the sands, rather than a real change difference in fluid content. Clearly, further improving the resolution of the data would reduce the uncertainty due to sand thickness, and integrating the results of the planned drilling programme would also improve the characterisation of the sands within the block.

Conclusions

Careful pre-processing to remove noise and multiple contamination, followed by high fidelity velocity model building and 3D pre-stack depth imaging has yielded a data volume suitable for accurate AVO and EI analysis.

The results show a characteristic and anomalous far-offset stack low elastic impedance (representative of Palaeocene hydrocarbon-bearing sandstones) within a depositional channel running SE from the MacCulloch field. A similar far-offset stack low elastic impedance zone also sits around the structurally high prospect in the NW of 15/25b. The far-offset stack low elastic impedance values can be rigorously tied to well data and to the elastic response characteristics of the neighbouring MacCulloch and Blenheim fields adding confidence to the interpretation of the low elastic impedance as being characteristic of hydrocarbon bearing Palaeocene sandstones.

Rock physics modelling on the oil-bearing well 15/25b-3 suggests that AVO and elastic inversion analysis should assist in the location of hydrocarbon-bearing Palaeocene sandstones.

The analysis results are unusually unambiguous because of the excellent well control, calibration at MacCulloch and Blenheim fields and the good quality of the seismic data. Therefore it seems unlikely that the low EI38 bodies are not indicating oil bearing sands, however this requires that a stratigraphic trapping mechanism must exist for many of the bodies identified.

References

Claerbout, J.F. [1992], Earth Soundings Analysis: PVI, Blackwell Scientific Publications.

Connolly, P. [1999], Elastic impedance. The Leading Edge, April, 438-452.

Hardy, P.B. [2003], High resolution tomographic MVA with automation, SEG/EAGE summer research workshop, Trieste.

Jones, I.F. [2003], A review of 3D preSDM velocity model building techniques First Break, v21, No.3, pp45-58.

Jones, I.F., Fruehn, J. [2003], Factors affecting frequency content in 3D preSDM imaging, : The Leading Edge, v22, No.2,.pp128-134.

Scorer, J., Fuller, N., Malcolm, J., Bruner, J. [2003], The MacCulloch Field: Improving reservoir characterisation through time-lapse analysis. Proceedings of the 6th Petroleum Geology Conference.

Simm, R.W, Kemper, M., Deo, J., [2002], AVO Impedance: A new attribute for Fluid and Lithology Discrimination, Petex Conference, London

Sugrue' M.J., Jones' I.F., Evans' E.J., Fairhead, S., Marsden, G., [2003], Velocity Estimation in Complex Chalk, SEG/EAGE summer research workshop, Trieste.

Acknowledgements

The authors wish to thank Oilexco North Sea Ltd, for kind permission to use their data, and to colleagues within Oilexco, Ikon Science, Troy-Ikoda and GXT for assistance and advice with this work.

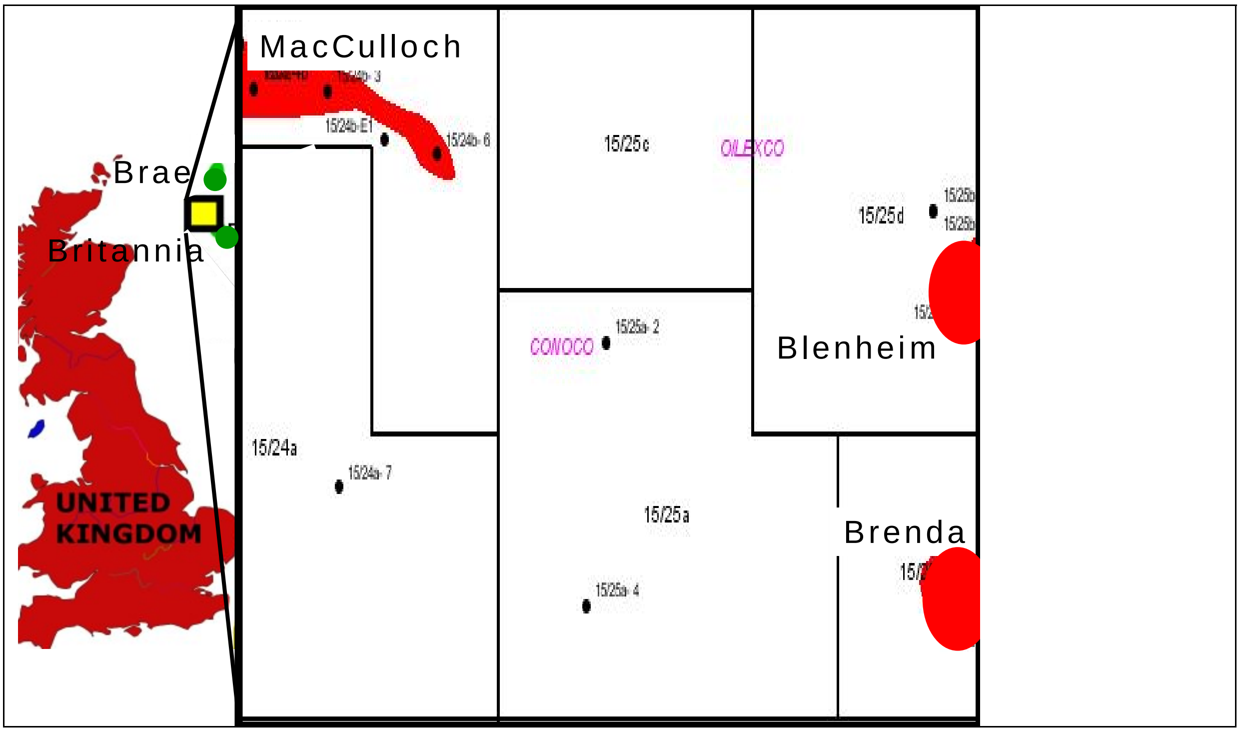

Figure 1. Location map showing position of new Brenda field.

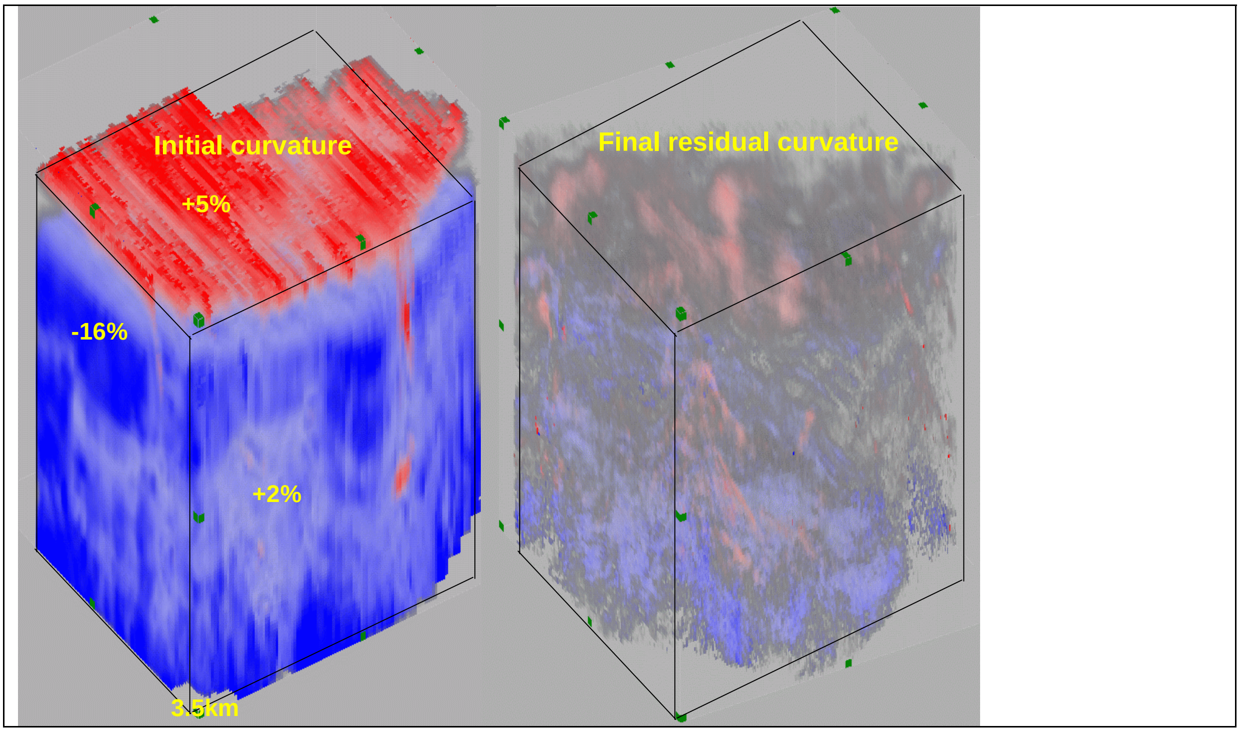

Figure 2. QC volumes from gridded tomographic inversion, showing residual velocity errors from the intial (left) and final (right) iterations.

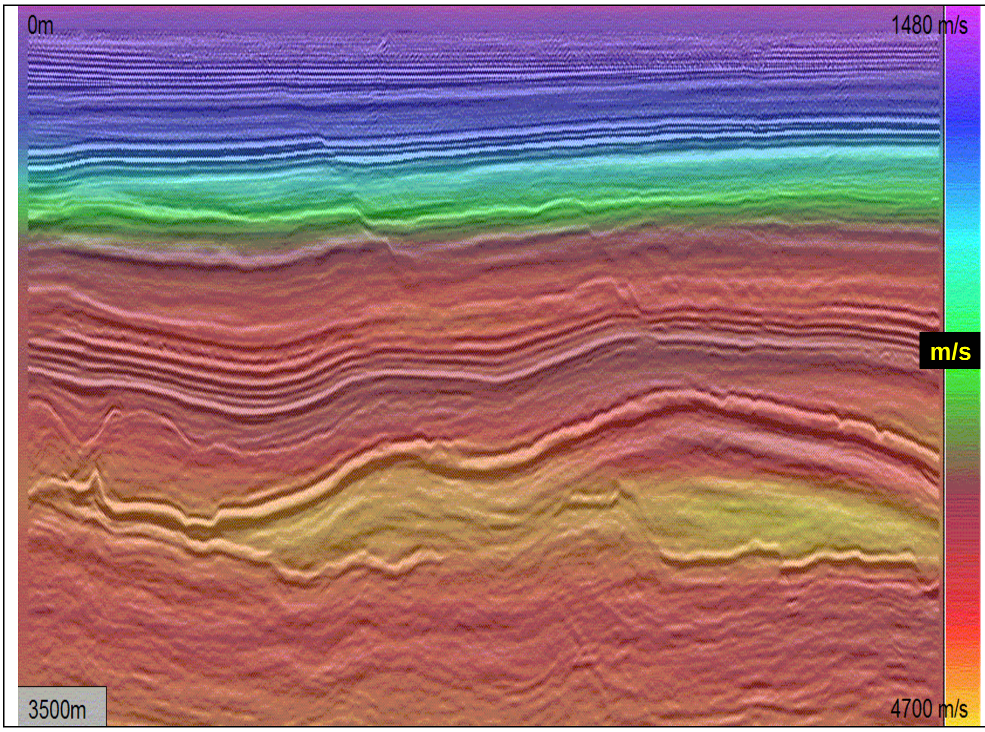

Figure 3. QC plot showing sample seismic overlaying the velocity field.

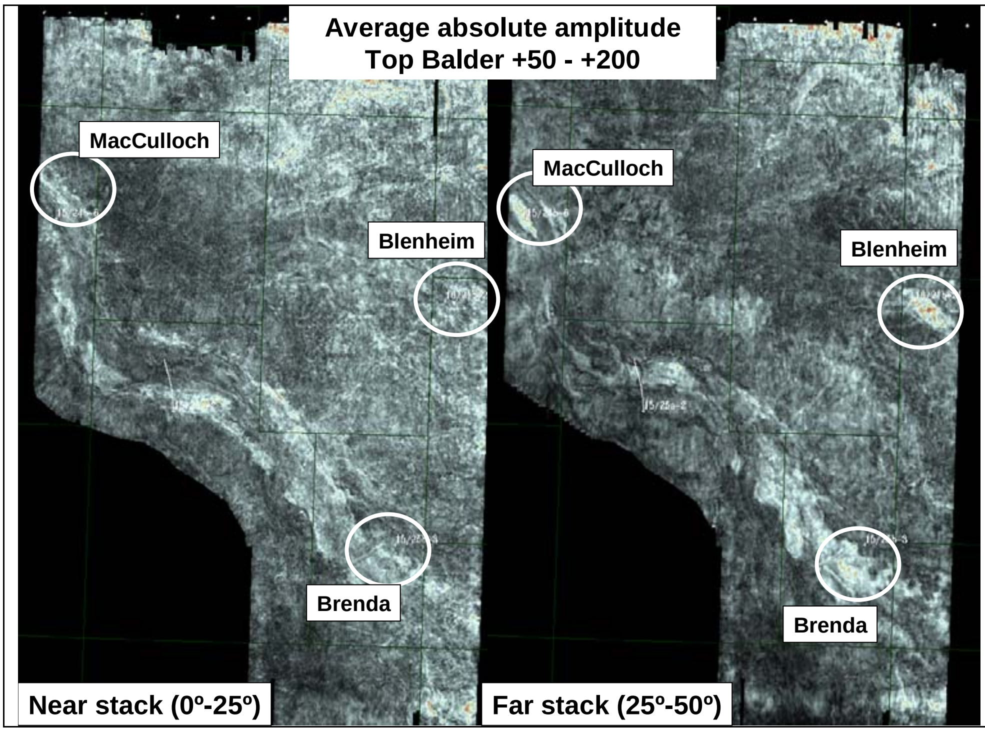

Figure 5. Amplitude maps near the Top Balder for the near and far angle stacks

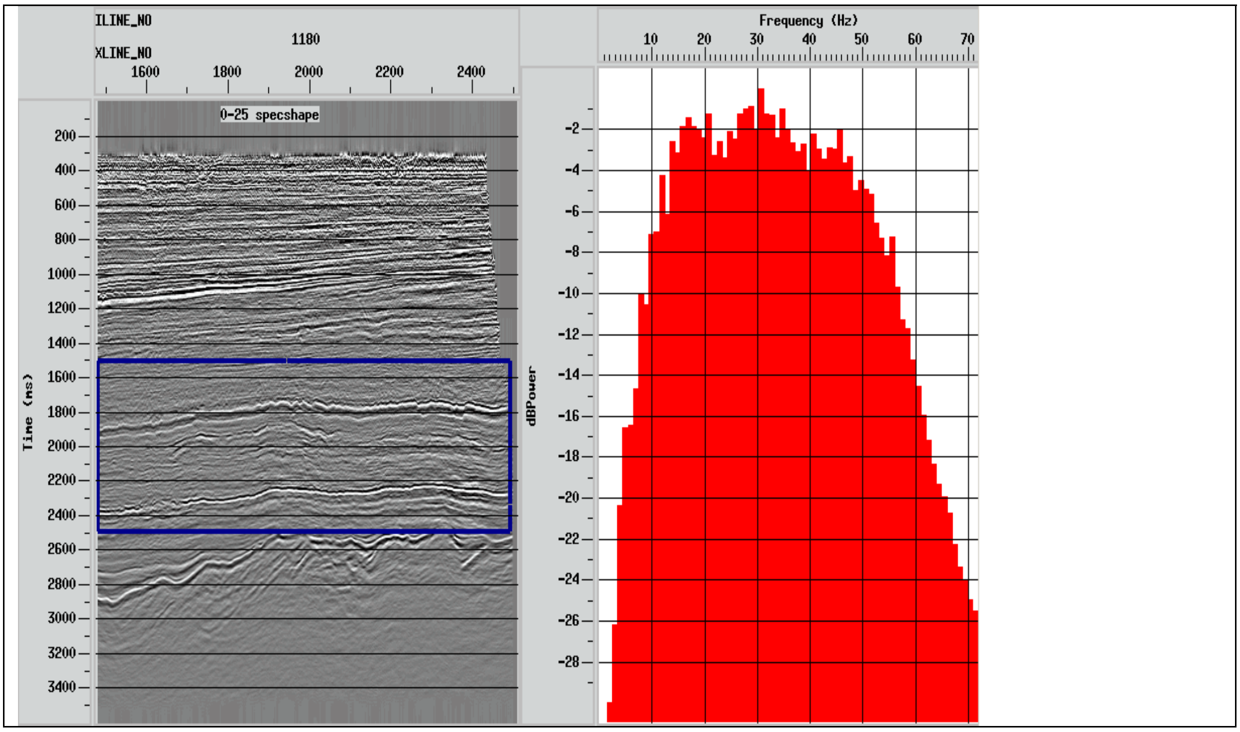

Figure 4a. Near angle stack and frequency spectrum

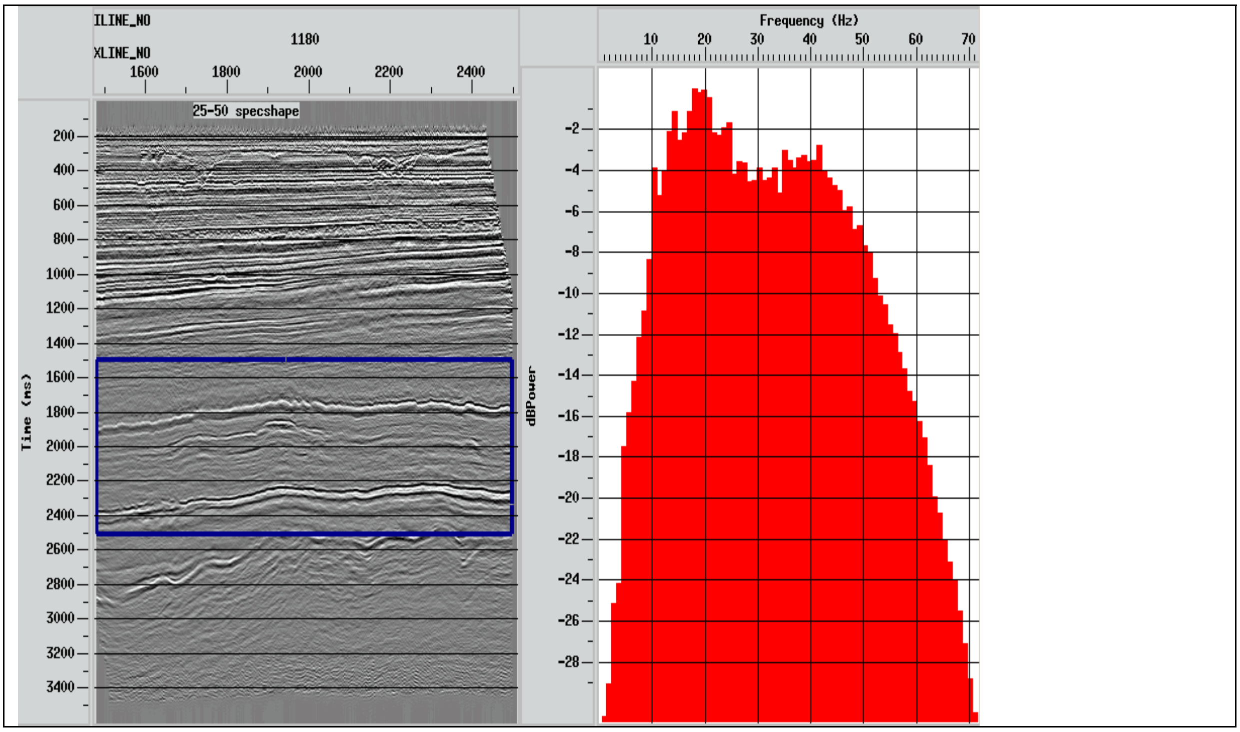

Figure 4b. Far angle stack and frequency spectrum

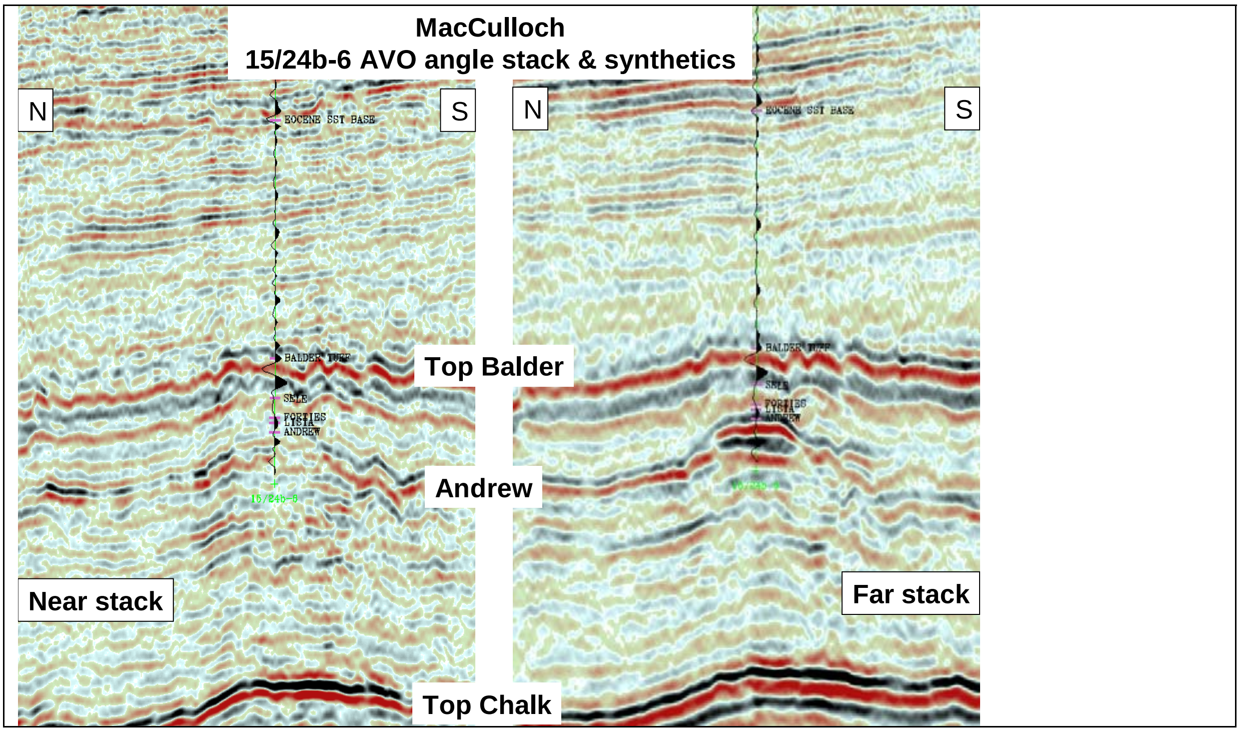

Figure 6. Near and far angle stacks over the MacCulloch field

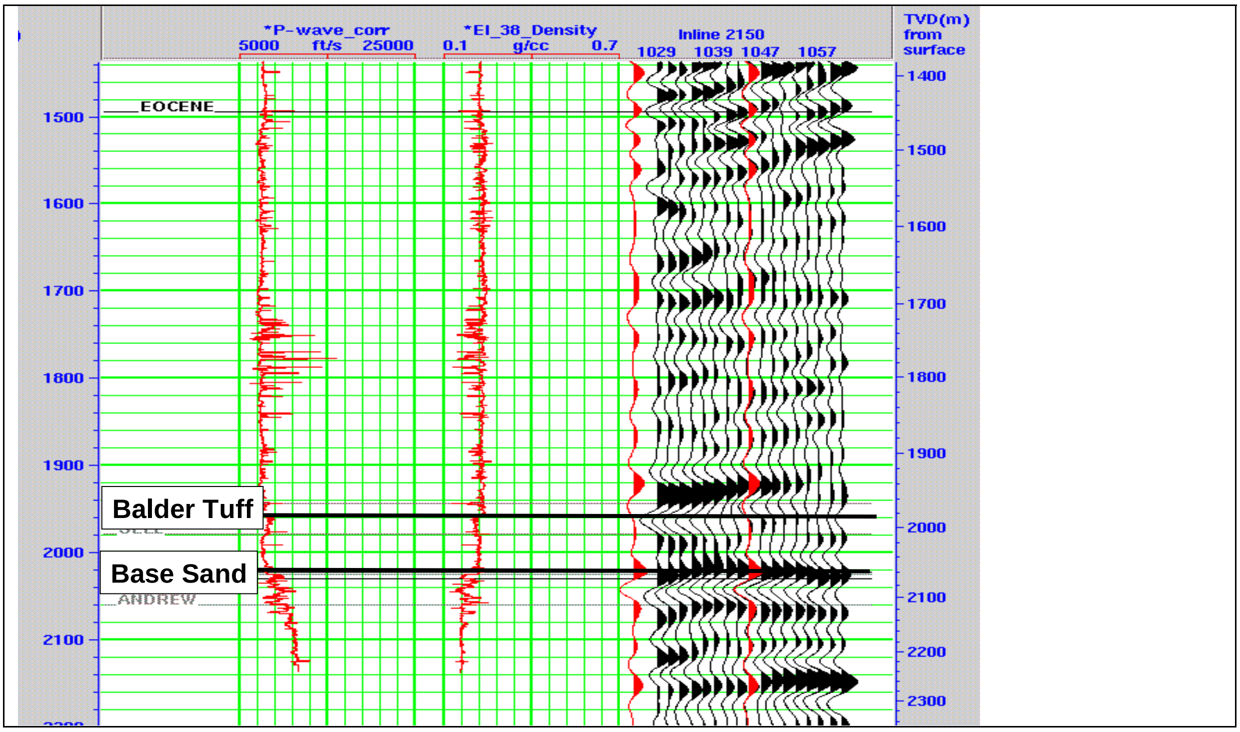

Figure 8. Far angle stack and predicted synthetic AVO response, for the 15/24b-6 well.

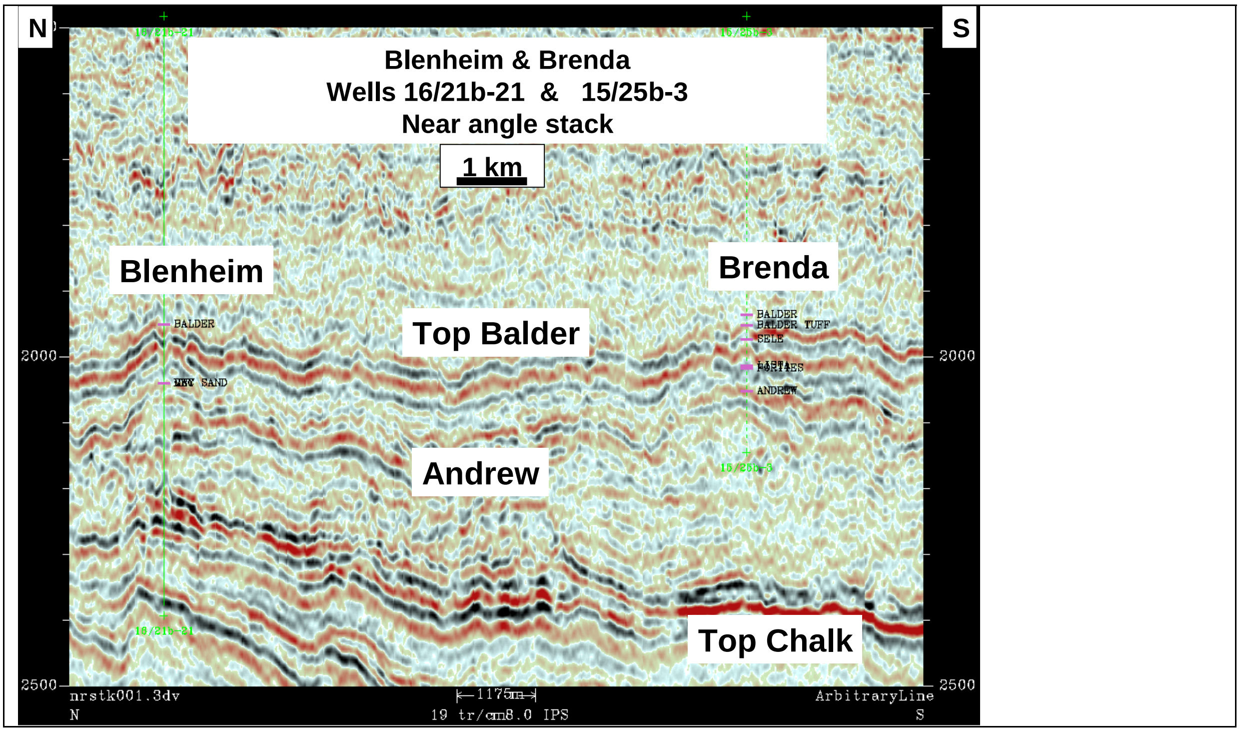

Figure 7a. Near angle stack over the Blenheim and Brenda fields

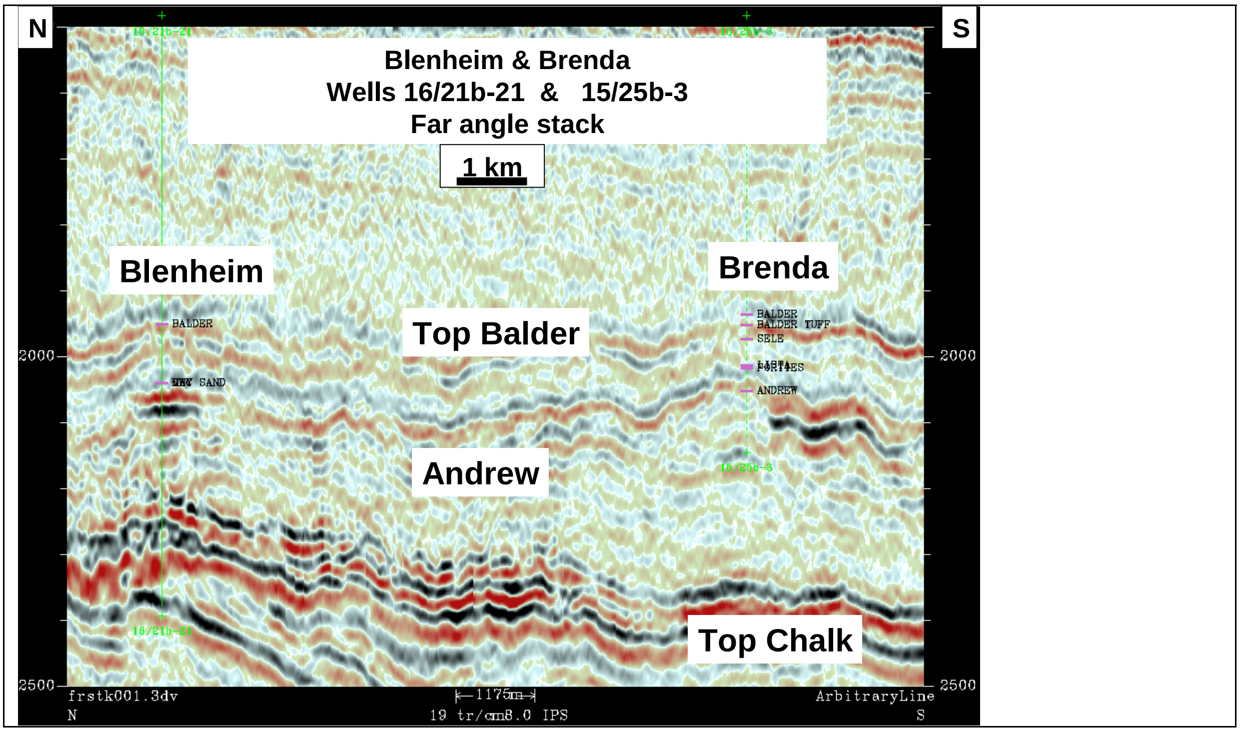

Figure 7b. Far angle stack over the Blenheim and Brenda fields

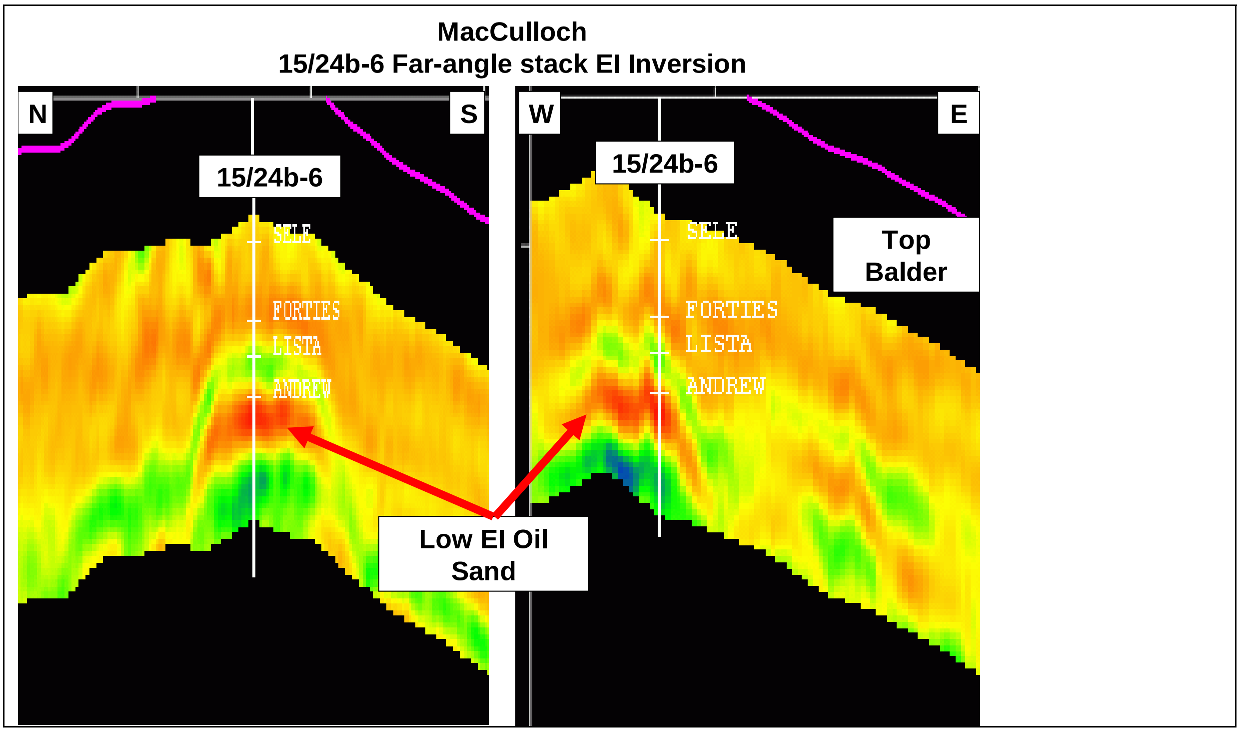

Figure 9. Far angle stack elastic impedance inversion for an inline and crossline through the 15/24b-6 well on the MacCulloch field. The well clearly penetrates the EI anomaly..

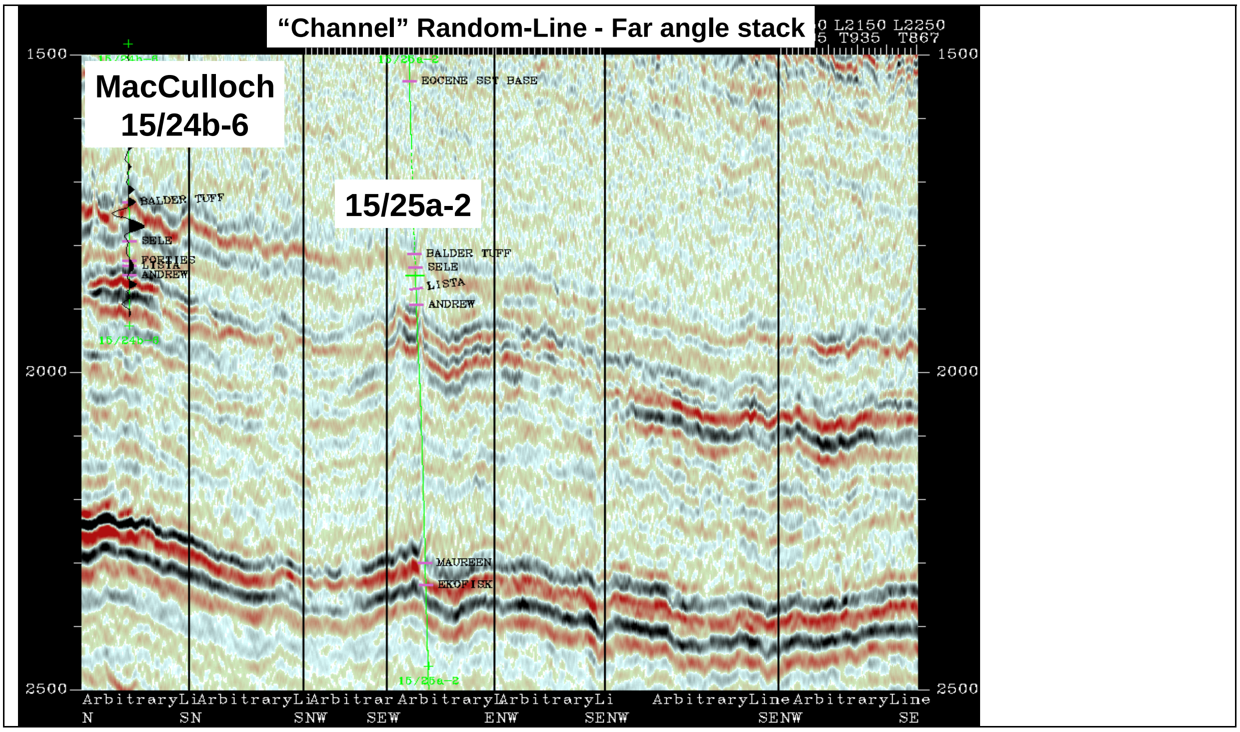

Figure 10. Far angle stack of a random line passing along the channel feature, indicating the location of the 15/25a-2 well.

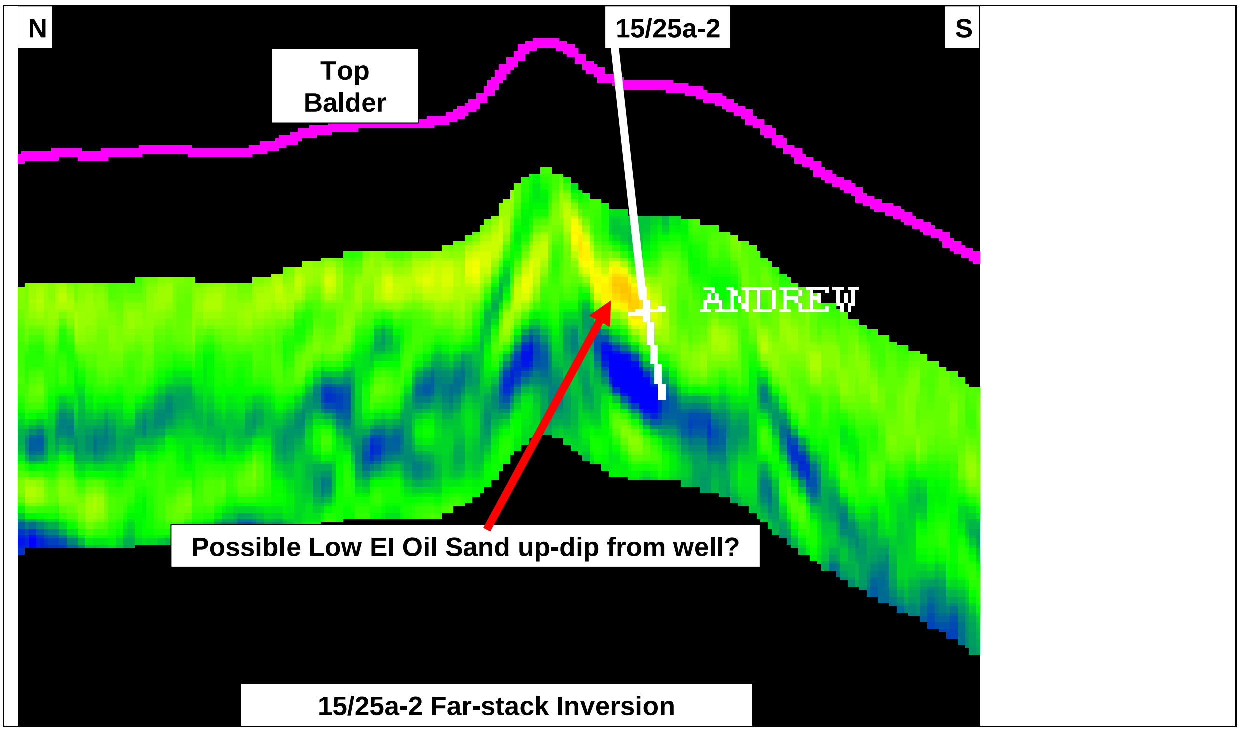

Figure 11. Far angle stack elastic impedance inversion through the unsuccessful 15/25a-2 well in the channel feature. The well clearly passes down-dip of the EI anomaly..

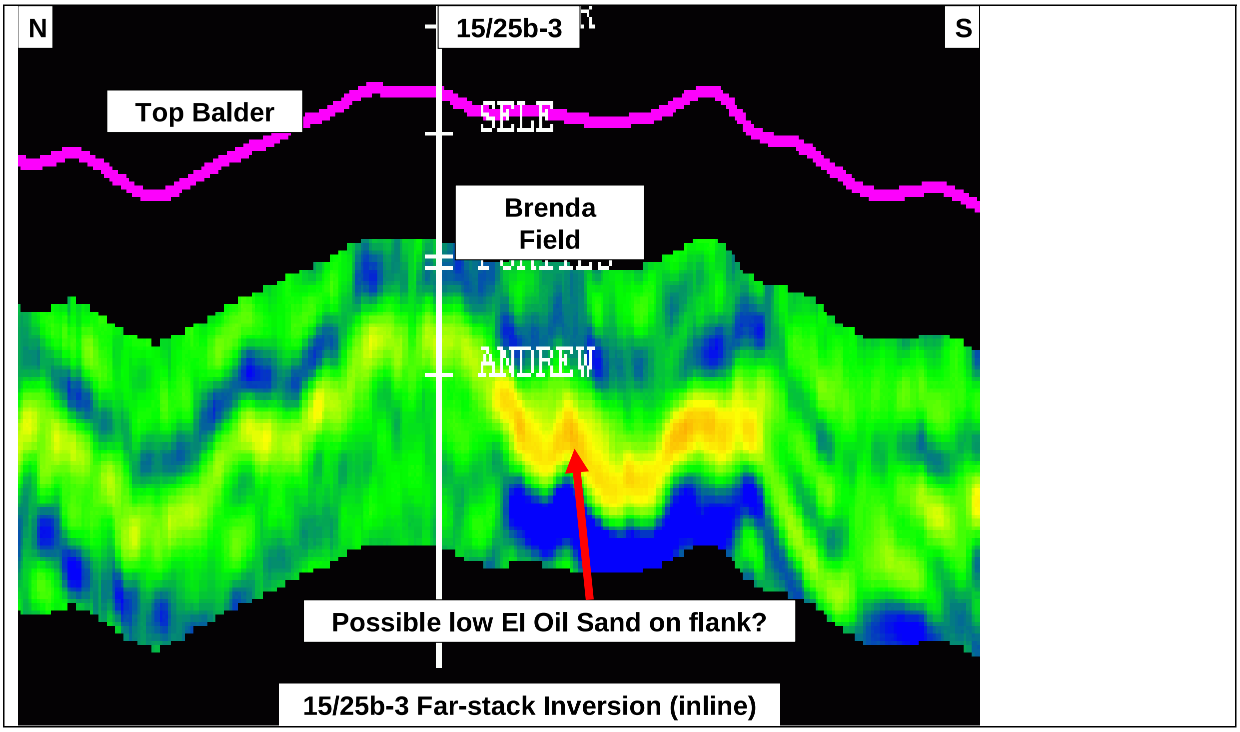

Figure 12a. Far angle stack elastic impedance inversion on a N-S inline in the channel feature. The 15/25b-3 Conoco well (which showed hydrocarbon potential) passes near the EI anomaly. The EI anomaly seen here is the newly defined Brenda field.

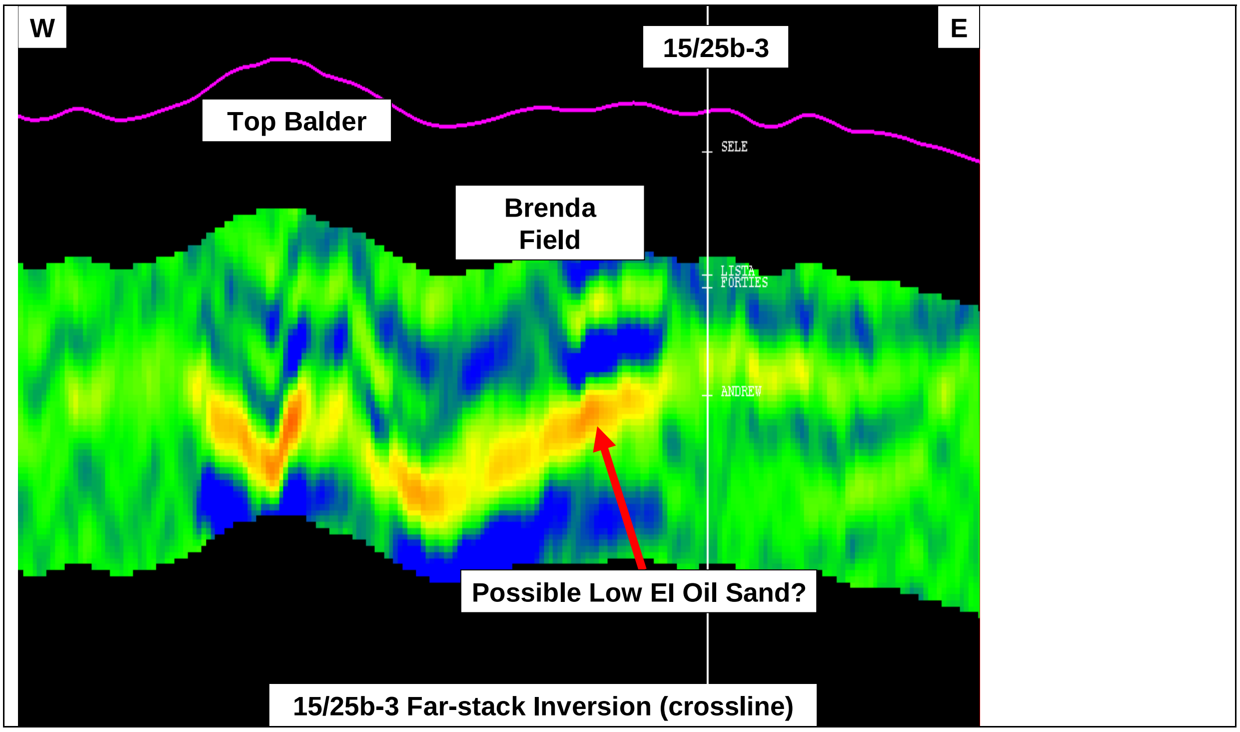

Figure 12b. Far angle stack elastic impedance inversion on a W-E crossline in the channel feature.

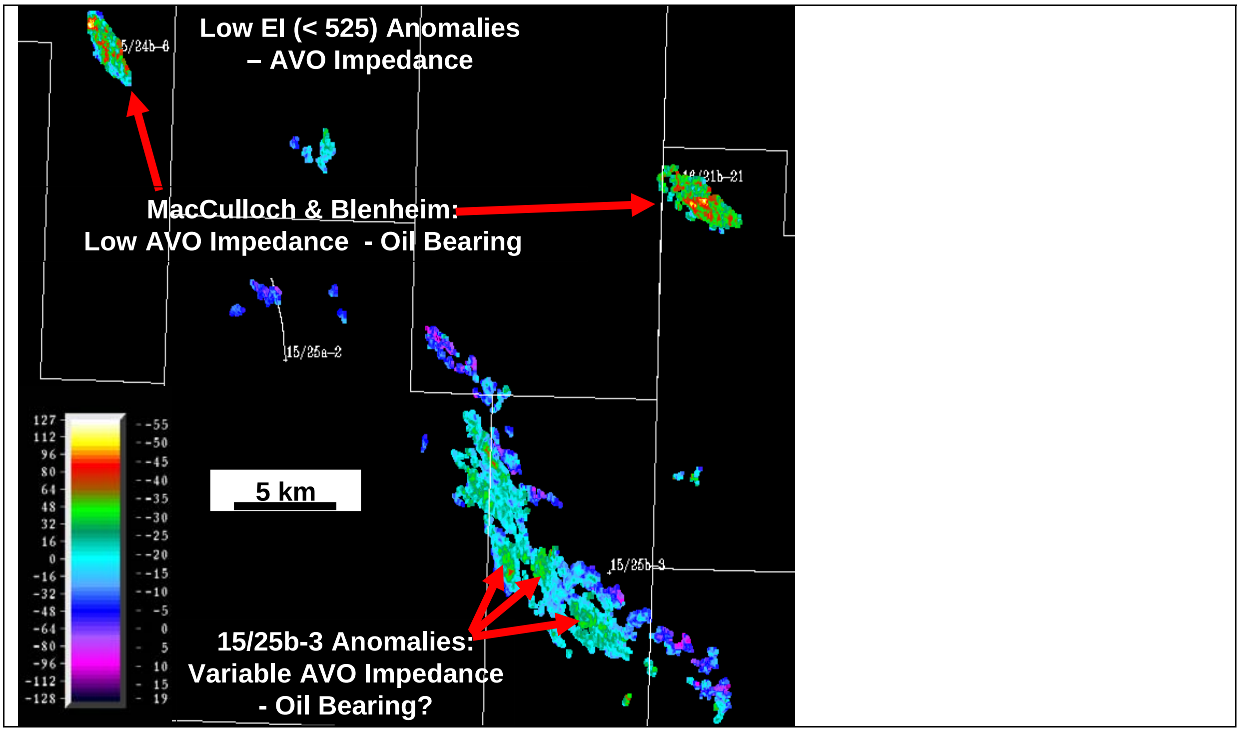

Figure 13. Far angle stack elastic impedance inversion result over the area. The voxels in the volume have been adjusted to only show EI values less then 525. The channel feature and the existing MacCulloch and Blenheim fields are clearly seen.